JOURNAL OF Materials CHEMISTRY

Determination of the magnetic structure at 10 K of $Mn_3Ta_2O_8$, and refinement of the crystal structure at 295 K, using neutron powder diffraction data

Jekabs Grins,*[a] Saeid Esmaeilzadeh,[a] Pedro Berastegui[a] and Sten Eriksson[b]

[a]*Department of Inorganic Chemistry, Arrhenius Laboratory, Stockholm University, SE-106 91 Stockholm, Sweden*
[b]*Studsvik Neutron Research Laboratory, SE-611 82 Nyköping, Sweden*

Received 18th March 1999, Accepted 26th April 1999

The Mn^{2+}-containing oxide $Mn_3Ta_2O_8$ crystallises in the space group $I4_1/a$ with $a=11.2728(2)$ and $c=9.8030(3)$ Å, and with a structure related to the cubic fluorite type. The compound is antiferromagnetic with a Néel temperature of 23 K. The magnetic structure at 10 K was determined from constant-wavelength ($\lambda=1.47$ Å) neutron powder diffraction (NPD) data and refined by the Rietveld method to $R_F=2.1\%$ and $S=1.3$ for 80 reflections with magnetic contributions at $2\theta\leqslant60^\circ$. The magnetic moments, of magnitude 4.01(2) μ_B, lie in the *ab* plane and are antiparallel with the (001) planes. The spin ordering is similar to that in the cubic fluorite structure of UO_2 but with 40% of the magnetic atoms replaced with non-magnetic Ta atoms. The non-magnetic crystal structure at 295 K was refined to $R_F=0.6\%$ using time-of-flight (TOF) NPD data, anisotropic thermal parameters and 1943 reflections with $d\geqslant0.55$ Å.

Introduction

This characterisation of $Mn_3Ta_2O_8$ forms part of a general study of the structures and properties of Mn–Ta oxides. The Mn–Ta–O system was initially investigated by Turnock at 1200 °C under various partial pressures of oxygen ranging from 10^{-17} to 1 atm.[1] Subsequently, we have determined the structures of the Mn^{2+}-containing compounds $Mn_{11}Ta_4O_{21}$,[2] $Mn_3Ta_2O_8$[3] and performed transmission electron microscopy (TEM) studies of the oxygen-deficient cubic fluorite $Mn_{0.6}Ta_{0.4}O_{1.65}$.[4] Preparations with metal contents of 50–80% Mn at 1000–1450 °C in air have further yielded a series of related incommensurate phases which are under investigation. Until now, the structure of one of these phases, with composition $Mn_{0.6}Ta_{0.4}O_{1.7+\delta}$, has been solved and refined from X-ray single-crystal data.[5]

The structure of $Mn_3Ta_2O_8$ was determined from synchrotron X-ray powder diffraction (XRPD) data.[3] It is related to the cubic MX_2 fluorite type and crystallises in the space group group $I4_1/a$ with $a=11.2728(2)$ Å$\approx\sqrt{5}a_f$ and $c=9.8030(3)$ Å$\approx2a_f$. The structure type is found to also be adopted by the compound $Ga_{3-x}In_{5+x}Sn_2O_{16}$,[6] $0.3<x1.6$. The magnetic susceptibility of $Mn_3Ta_2O_8$ shows a sharp maximum at 23 K and a Curie–Weiss behaviour at higher temperatures, with $\mu_{eff}=5.7(1)$ μ_B per Mn atom, indicating that $Mn_3Ta_2O_8$ is antiferromagnetic below 23 K. Electron diffraction patterns, however, showed the presence of superstructure reflections which correspond to a primitive unit cell with $a'=a$ and $c'=6c$. The synchrotron XRPD data exhibited no corresponding reflections.

NPD data for $Mn_3Ta_2O_8$ were collected with two objectives. Data were recorded at room temperature in the hope of obtaining further information about the indicated superstructure, since the electron diffraction superstructure reflections could originate from a distortion of the O atom sublattice and therefore contribute little to an XRPD pattern. We also collected data at 10 K in order to determine an expected ordered magnetic structure.

Experimental

Samples of $Mn_3Ta_2O_8$ were prepared by solid state reaction as described in ref. 3. TOF NPD data for $Mn_3Ta_2O_8$ were collected at room temperature on the Polaris diffractometer at the UK spallation neutron source ISIS, Rutherford Appleton Laboratory, and the normalised patterns were corrected for sample absorption effects. NPD data at 10 K were collected at the Swedish research reactor R2 in Studsvik between 4 and 140° in 2θ ($\lambda=1.47$ Å). The Rietveld structure refinements were made with the GSAS program.[7]

Results

Refinement of the room temperature crystal structure

A Rietveld structure refinement of $Mn_3Ta_2O_8$, with 18 positional parameters, 8 isotropic thermal displacement parameters, 1943 reflections with *d* values between 0.55 and 3.2 Å and a total of 58 refined parameters, converged with $\chi^2=1.4$ and $R_F=1.1\%$. Allowance for 40 anisotropic thermal parameters in a corresponding refinement yielded an improved and very good fit between the observed and calculated patterns, with $\chi^2=0.95$ and *R*-values[8] of $R_{wp}=1.60\%$, $R_p=3.57\%$, Dwd = 0.912 and $R_F=0.6\%$. The obtained atomic parameters are given in Table 1, together with those determined from the

Table 1 Atomic coordinates and thermal parameters for $Mn_3Ta_2O_8$

Atom	Site	*x*	*y*	*z*	U_{eq}/Å^2
Ta	16(*f*)	0.42179(7)	0.05600(7)	0.1299(1)	0.0021[a]
		0.42257(7)	0.05661(9)	0.1300(1)	0.00641(2)[b]
Mn1	16(*f*)	0.3794(2)	0.0488(2)	0.5990(2)	0.0126
		0.3780(5)	0.0505(3)	0.5949(3)	0.0077(1)
Mn2	4(*a*)	0	1/4	1/8	0.0135
		0	1/4	1/8	0.0073(2)
Mn3	4(*b*)	0	1/4	5/8	0.0051
		0	1/4	5/8	0.0071(2)
O1	16(*f*)	0.3718(1)	0.2016(1)	0.2101(1)	0.0078
		0.362(1)	0.198(1)	0.221(1)	0.0043(3)
O2	16(*f*)	0.4633(1)	0.8965(1)	0.0187(1)	0.0053
		0.460(1)	0.893(1)	0.013(1)	0.0043(2)
O3	16(*f*)	0.1973(1)	0.3080(1)	0.9996(1)	0.0075
		0.196(1)	0.312(1)	0.997(1)	0.0056(3)
O4	16(*f*)	0.3168(1)	0.9626(1)	0.2423(1)	0.0078
		0.310(1)	0.961(1)	0.243(1)	0.0048(2)

[a]From TOF NPD data. [b]From synchrotron XRPD data.[3]

Table 2 Anisotropic thermal displacement parameters ($Å^2 \times 100$), defined by $T = \exp[-2\pi^2(h^2a^{*2}U_{11} + \ldots + 2hka^*b^*U_{12} + \ldots)]$, for $Mn_3Ta_2O_8$ from TOF NPD data

Atom	U_{11}	U_{22}	U_{33}	U_{12}	U_{13}	U_{23}
Ta	0.25(3)	0.13(3)	0.25(3)	0.04(3)	0.01(3)	−0.02(3)
Mn1	1.42(8)	1.09(7)	1.25(9)	−0.23(7)	−0.74(6)	0.78(7)
Mn2	1.54(11)	1.54	1.0(2)	0	0	0
Mn3	0.36(8)	0.36	0.8(1)	0	0	0
O1	0.84(5)	0.39(4)	1.12(5)	0.20(3)	−0.21(4)	−0.34(3)
O2	0.62(5)	0.47(4)	0.49(4)	0.04(4)	0.40(3)	0.08(4)
O3	1.10(4)	0.49(4)	0.65(4)	0.14(4)	−0.44(4)	−0.24(3)
O4	0.96(5)	0.82(4)	0.55(4)	−0.36(4)	0.11(4)	0.31(4)

synchrotron X-ray data given in ref. 3. The thermal parameters and selected bond distances and angles are given in Tables 2 and 3, respectively. Note that the O atoms for the Mn2–O distances are erroneously labelled in Table 3 of ref. 3. In comparison with the XRPD data, the NPD data provide a roughly ten-fold better determination of the locations of the O atoms and thus validate the arrangement of the previously determined structure. The atomic parameters from the two data sets appear to differ significantly, however, with the largest difference found for the z coordinate of Mn1 corresponding to 14 e.s.d.s. It is clear that the e.s.d. values in both data sets are probably underestimated by factors of roughly 2–4, considering that serial correlation[9] is present, as quantified by the Durbin–Watson d statistic (Dwd), which has not been accounted for. However, even if the e.s.d.s are multiplied by three, there are some differences that correspond to more than three e.s.d.s. We have no good explanation for this discrepancy.

The diffraction pattern exhibited no extra reflections that could be ascribed to the superstructure implied by the electron diffraction studies (*cf.* concluding remarks).

Determination and refinement of the magnetic structure at 10 K

The constant-wavelength NPD pattern collected at 10 K exhibited three strong reflections of purely magnetic origin: 110, 002 and 310. The two reflections 110 and 310 do not conform with the glide-plane that is present in the main structure, and the 002 reflection is not compatible with a 4_1 axis, whereas they all agree with the reflection conditions for an I-centered unit cell. A satisfactory model for the magnetic structure was arrived at by trial and error. The space group $I\bar{1}$ was used, and atomic coordinates and thermal parameters were constrained to those of the non-magnetic structure. The model was refined with reflections in the range $2\theta = 10$–140° and magnetic contributions to reflection intensities for $2\theta \leqslant 60^\circ$ ($d \geqslant 1.48$ Å) were allowed for. A total of 67 parameters were refined, including 18 positional and 8 isotropic thermal parameters. The fit between the observed and calculated NPD

Table 3 Bond distances (Å) and bond angles (degrees) for $Mn_3Ta_2O_8$

Ta–O1	1.905(2)	Mn1–O3	2.003(2)	Mn2–O1	2.236(1) × 4
Ta–O4	1.930(1)	Mn1–O3	2.071(2)	Mn2–O3	2.624(1) × 4
Ta–O3	1.932(1)	Mn1–O1	2.155(2)	mean 2.43	
Ta–O2	2.021(1)	Mn1–O1	2.493(2)		
Ta–O4	2.032(1)	Mn1–O2	2.508(2)	Mn3–O2	1.997(1) × 4
Ta–O2	2.154(1)	Mn1–O4	2.514(2)	mean 2.00	
		Mn1–O4	2.622(2)		
mean 2.00		mean 2.34			

Mn1–O1–Mn1	98.09(8)
Mn1–O3–Mn1	108.0(1)
Mn1–O4–Mn1	79.81(3)
Mn1–O1–Mn2	100.55(6)
	103.03(7)
Mn1–O3–Mn2	93.40(7)
	102.97(7)
Mn1–O2–Mn3	113.78(6)

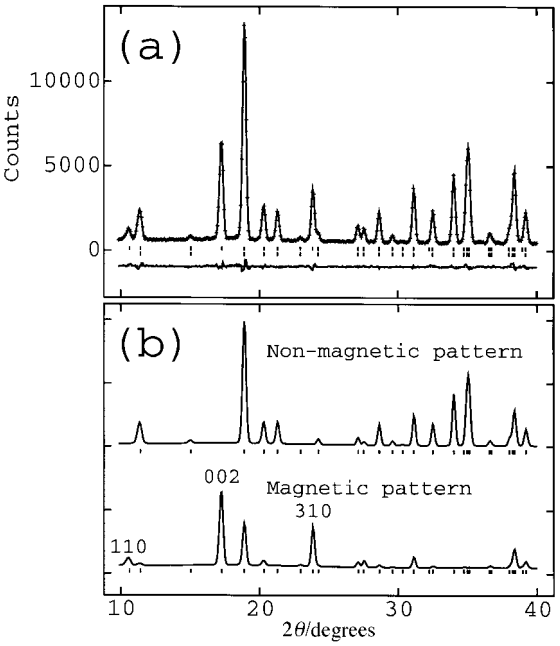

Fig. 1 (a) Observed (crosses), calculated (solid line) and difference (bottom) NPD patterns recorded at 10 K for $Mn_3Ta_2O_8$ in the range $2\theta = 10$–40°. (b) Calculated NPD patterns for the non-magnetic and magnetic structures.

patterns is shown for $2\theta = 10$–40° in Fig. 1(a) and calculated patterns for purely non-magnetic and magnetic structures are given in Fig. 1(b). The obtained atomic coordinates were not significantly different from those given in Table 1. Only one parameter was used for the magnetic structure, namely a collective magnetic moment for all three crystallographically different Mn atoms, with a refined value of 4.01(2) μ_B. The residuals were $\chi^2 = 1.75$, $R_{wp} = 4.24\%$, $R_p = 3.35\%$, Dwd = 1.37, $R_F = 1.0\%$ for the main structure (666 reflections) and $R_F = 2.1\%$ for the magnetic structure (80 tetragonal reflections). A corresponding refinement with individual magnetic moments for the three different types of Mn atoms yielded only marginally smaller residuals and μ_{eff} values of 3.91(3), 4.17(8) and 4.04(8) μ_B for Mn1, Mn2 and Mn3, respectively.

Description of the crystal and magnetic structures

We will now give an alternative description of the crystal structure of $Mn_3Ta_2O_8$ to those given in ref. 3. The O atom coordination polyhedra around the metals and the thermal vibration ellipsoids are illustrated in Fig. 2. The Ta atoms are coordinated by a distorted octahedron of O atoms. The Mn1 atoms are coordinated by seven O atoms at distances between 2.003(2) and 2.622(2) Å, and the coordination polyhedron can be idealised as a cube with one corner missing. The Mn2 atoms are 4+4 coordinated, with a resulting eight-coordinate polyhedron that may be described as a distorted cube, and Mn3 is tetrahedrally coordinated.

The metal atoms are nearly in cubic close packing and the positional shifts from the metal array found in a cubic fluorite structure are small. A polyhedral illustration of the Mn atom arrangement, of relevance to the magnetic structure, is given in Fig. 3(a) together with an idealised arrangement for a corresponding cubic fluorite type structure. The Ta atoms (not shown in Fig. 3) are located at positions that are displaced from the Mn1 positions by $z \approx 1/2$. The structure thus contains strings of Mn1–vacancy–Ta–vacancy polyhedra along the c axis. The Mn2 and Mn3 atoms are found in the channels between the Mn1–Ta strings of polyhedra. A visualisation of the connections between the different Mn–O polyhedra is aided by noting that the site symmetry for the Mn2 and Mn3 atoms is $\bar{4}$.

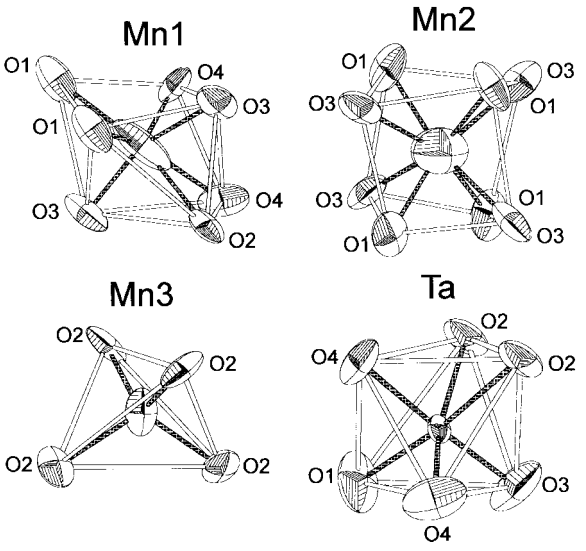

Fig. 2 Coordination polyhedra in $Mn_3Ta_2O_8$.

Probable pathways for magnetic couplings between the Mn atoms can be found by inspection of the observed Mn–O distances. A strong coupling can be expected between the Mn1 atoms in the helical strings along the *c* axis, shown in Fig. 3, which are bridged by O3 atoms at short distances and, additionally, by O4 atoms. The Mn1–O polyhedra in these strings are further linked to those in adjacent strings *via* corner-sharing of O1 atoms. They are also interconnected by

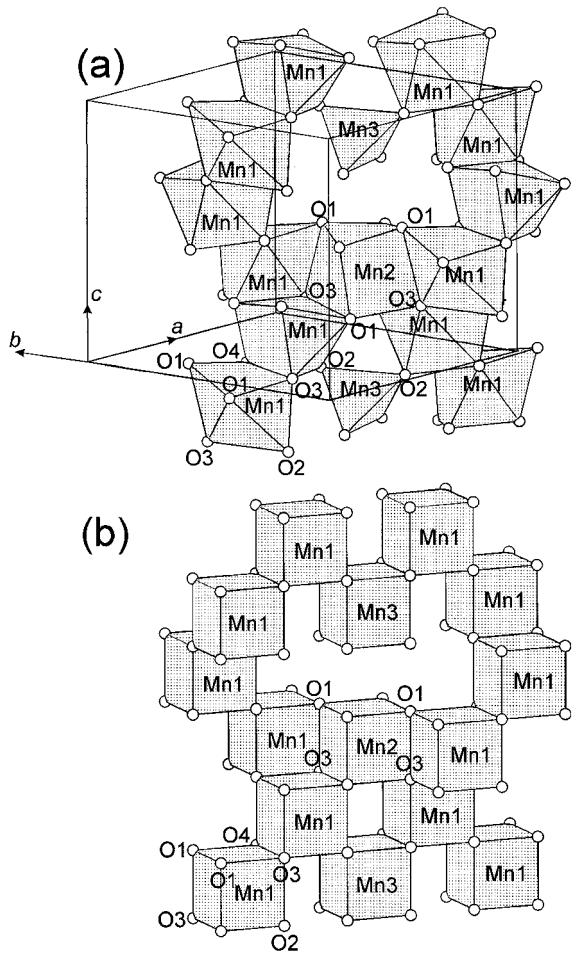

Fig. 3 (a) A polyhedral illustration of the Mn atom arrangement in the structure of $Mn_3Ta_2O_8$. (b) A corresponding arrangement for a hypothetical cubic fluorite type structure.

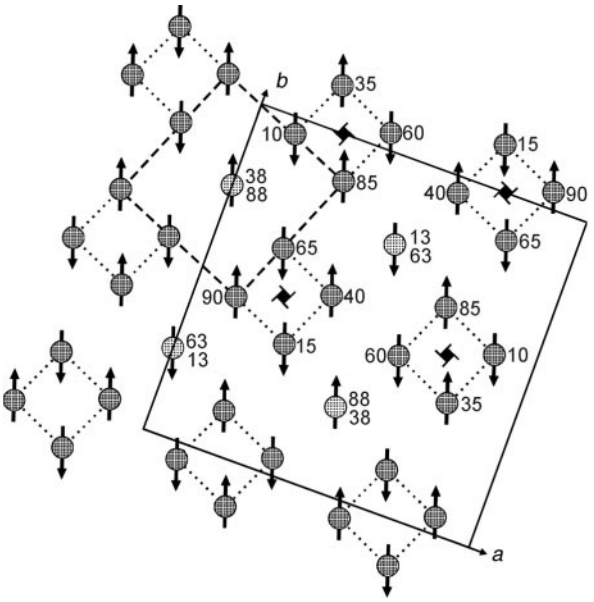

Fig. 4 An illustration of the magnetic structure of $Mn_3Ta_2O_8$ at 10 K, projected on the *ab* plane. The Mn1 atom positions are shown by darker shaded circles and those for Mn2 and Mn3 atoms by lighter shaded circles. The numbers designate the fractional coordinates of the Mn atoms along *c*, multiplied by 100. The Mn1 atoms that are symmetry related by 4_1 axes are connected by dotted lines. A subcell corresponding to a cubic fluorite type structure is outlined by dashed lines.

the Mn2 and Mn3 atoms, which both connect to four strings of Mn1 polyhedra *via* the O2 and O1, O3 atoms, respectively.

The antiferromagnetic structure model for $Mn_3Ta_2O_8$ is illustrated in Fig. 4 projected on the *ab* plane. The magnetic moments accordingly lie in the *ab* plane with a refined value of 4.01(2) μ_B. The directions of the moments within the *ab* plane cannot be inferred from the powder data.[10] No alternative models could be found that agreed with the observed intensities of the magnetic Bragg peaks. The colour symmetry is $I\underline{4}_1/\underline{a}$, *i.e.* spin reversals accompany the symmetry operations of the *a* glide and 4_1 axis. Layers parallel with (001) [and also with (310) and (1$\bar{3}$0)] contain Mn atoms with parallel moments, and spins are reversed in alternating layers, situated at $z = 1/8$, 3/8, 5/8 and 7/8. Each such layer contains four Mn1, one Mn2 and one Mn3 atoms (plus four non-magnetic Ta atoms) per unit cell. A subcell corresponding to a cubic fluorite type structure is outlined by dashed lines in Fig. 4.

Conclusions

The refinement of the crystal structure of $Mn_3Ta_2O_8$, representing a new type of structure related to that of fluorite, from NPD data gives an improved determination of the light O atom positions and, as a result, also of the metal–oxygen atom distances. The data set contained no reflections from the superstructure as seen in the electron diffraction patterns.[3] The only explanation we have at present is that the superstructure domains might be too small to give detectable Bragg peaks in an NPD or XRPD pattern, but of sufficient size to give relatively sharp, but in comparison broader, electron diffraction spots.

The ordering of magnetic moments found in $Mn_3Ta_2O_8$ at 10 K is similar to that in the antiferromagnetic structure of the cubic fluorite UO_2,[11] where spins in the (001) planes are antiparallel. Two major differences between the structures are, however, that the former is not cubic and contains non-magnetic Ta atoms that occupy 40% of the metal atom sites in an ordered manner.

Acknowledgements

Prof. M. Nygren is thanked for support and valuable discussions. This work has been financially supported by the Swedish Natural Science Foundation.

References

1 A. C. Turnock, *J. Am. Ceram. Soc.*, 1966, **49**, 382.
2 J. Grins and A. Tyutyunnik, *J. Solid State Chem.*, 1998, **137**, 276.
3 S. Esmaeilzadeh, J. Grins and A. Fitch, *J. Mater. Chem.*, 1998, **8**, 2493.
4 S. Esmaeilzadeh, J. Grins and A.-K. Larsson, *J. Solid State Chem.*, in press.
5 S. Esmaeilzadeh, J. Grins and S. Lidin, unpublished results.
6 D. D. Edwards, T. O. Mason, W. Sinkler, L. D. Marks, F. Goutenoire and K. R. Poeppelmeir, *J. Solid State Chem.*, 1998, **140**, 242.
7 A. C. Larson and R. B. Von Dreele, Los Alamos National Laboratory Report No. LA-UR-86–748, 1987.
8 *The Rietveld Method*, *IUCr Monographs on Crystallography 5*, ed. R. A. Young, Oxford University Press, Oxford, 1993, p. 22.
9 J.-F. Bérar and P. Lelann, *J. Appl. Crystallogr.*, 1991, **24**, 1.
10 G. Shirane, *Acta Crystallogr.*, 1959, **12**, 282.
11 J. Faber, Jr. and G. H. Lander, *Phys. Rev. B: Condens. Matter.*, 1976, **14**, 1151.

Paper 9/02149C